



Long-term river discharge and multidecadal climate variability inferred from varved sediments, southwest Alaska

Claire A. Kaufman^a, Scott F. Lamoureux^{a,*}, Darrell S. Kaufman^b

^a Department of Geography, Queen's University, Kingston, ON, K7L 3N6, Canada

^b School of Earth Sciences and Environmental Sustainability, Northern Arizona University, Flagstaff, AZ, USA 86011–4099

ARTICLE INFO

Article history:

Received 15 April 2011

Available online 1 June 2011

Keywords:

Varves

Southwest Alaska

Discharge

Climate variability

Pacific Decadal Oscillation

North Pacific Index

Aleutian Low

ABSTRACT

Sedimentological analyses of 289 years (AD 1718–2006) of varved sediment from Shadow Bay, southwest Alaska, were used to investigate hydroclimate variability during and prior to the instrumental period. Varve thicknesses relate most strongly to total annual discharge ($r^2 = 0.75$, $n = 43$, $p < 0.0001$). Maximum annual grain size depends most strongly on maximum spring daily discharge ($r^2 = 0.63$, $n = 43$, $p < 0.0001$) and maximum annual daily discharge ($r^2 = 0.61$, $n = 43$, $p < 0.0001$), while varve thickness is poorly correlated with maximum annual grain size ($r^2 = 0.004$, $n = 287$, $p = 0.33$). Relations between varve thickness and annual climate variables (temperature, precipitation, North Pacific (NP) and Pacific Decadal Oscillation (PDO) indices) are insignificant. On multidecadal timescales, however, regime shifts in varve thickness and total annual discharge coincide with shifts in NP and PDO indices. Periods with increased varve thickness and total annual discharge were associated with warm PDO phases and a strengthened Aleutian Low. The varve-inferred record of PDO suggests that any periodicity in the PDO varied over time, and that the early 19th century marked a transition to a more frequent or detectable shifts.

© 2011 University of Washington. Published by Elsevier Inc. All rights reserved.

Introduction

Understanding climate-forcing mechanisms on multidecadal timescales is limited by short and spatially restricted regional hydrometeorological records. Annually laminated (varved) lake sediments provide an annual to sub-annual record of the hydroclimatic conditions that extend beyond the instrumental period. Numerous studies have used varves to reconstruct past environmental change, including air temperature (e.g. Desloges, 1994; Menounos et al., 2005), precipitation (e.g. Østrem and Olsen, 1987; Wohlfarth et al., 1998; Lamoureux, 2000), glacial melt (e.g. Leonard, 1997; Menounos, 2006), and river discharge (Sander et al., 2002). In regions with complex hydroclimate dynamics, the relations between mean climate variables and varve characteristics are not necessarily straightforward (Leemann and Niessen, 1994; Gilbert, 2003). Complex varve-climate relations can be interpreted through detailed studies of internal varve features that record hydroclimate variability on subannual timescales (e.g. Gilbert et al., 2006; Schiefer et al., 2006; Cockburn and Lamoureux, 2007; Menounos and Clague, 2008).

This paper presents a 289-year-long, subannual record of hydroclimatic change from Shadow Bay, Lake Chaeukuktuli, in southwest Alaska. The study focuses on linking varve characteristics to regional hydroclimatic records in order to understand factors controlling varve

formation, and to interpret the varve record beyond the length of instrumental records. Given the interest in climate change in the North Pacific on multidecadal timescales (e.g. Mantua et al., 1997; Zhang et al., 1997), this study addresses multidecadal shifts in varve characteristics and their association with modes of North Pacific climate variability including the Aleutian Low (Rodionov et al., 2007) and the Pacific Decadal Oscillation (Mantua and Hare, 2002).

Study Site

Shadow Bay (96 m above sea level (asl), 60° 00.96'N, 159° 18.22'W) is situated in a large, glacially eroded valley along the steep northeastern front of the Ahklun Mountains, ~140 km north of Bristol Bay, Alaska (Fig. 1A). The 4.3 km² bay forms the western inflow sub-basin of Lake Chaeukuktuli and is isolated from the main body of the lake by a c. 2-m-deep sill. Shadow Bay itself comprises two sub-basins that are 69 and 59 m deep (Fig. 1B). Mountains within the 125 km² watershed reach 1500 m asl and in the early 1970's, ~4% of the watershed was covered by small glaciers. Water and sediment are delivered to Shadow Bay primarily by a braided channel at the north end of the basin.

Climate in the region is transitional between maritime and continental regimes (National Oceanographic and Atmospheric Administration (NOAA), 1980). The interplay between these systems is manifested through intense storm activity and rapid temperature changes (Neal et al., 2002), and is strongly influenced by the Aleutian Low, a principal feature of atmospheric circulation in the Northern

* Corresponding author. Fax: +1 613 533 6122.

E-mail address: scott.lamoureux@queensu.ca (S.F. Lamoureux).

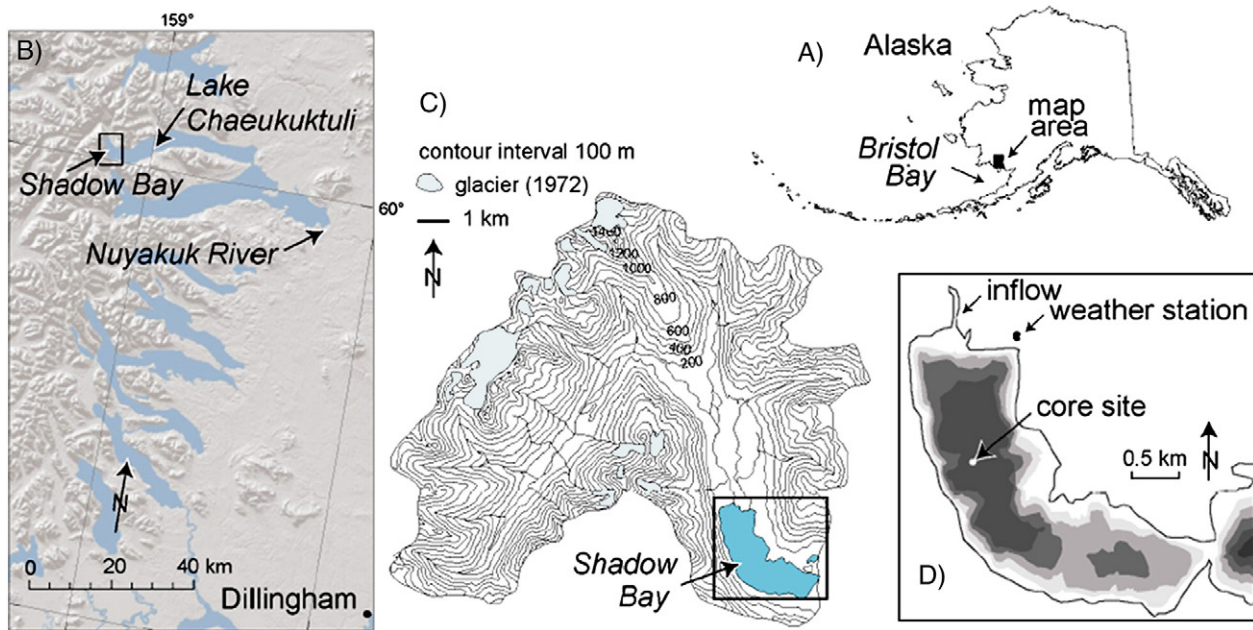


Figure 1. (A) Location of study area in Alaska and the (B) location of Shadow Bay, Lake Chaeukuktuli, and the Nuyakuk River gauging station (Station ID 15302000, 59° 56.08'N, 158° 11.16'W) within the Ahklun Mountains, southwest Alaska. (C) Watershed map of for Shadow Bay including glacier cover, and (D) bathymetric map of Shadow Bay showing core site. Bathymetric contours at 15 m intervals and were generated from 20 km of sounding transects.

Hemisphere during the winter (Trenberth and Hurrell, 1994). The Aleutian Low is centred near the Aleutian Islands, although its position and intensity may vary considerably on monthly to interdecadal timescales (Rodionov et al., 2005, 2007). Decadal regime shifts in the Aleutian Low have been associated with the Pacific Decadal Oscillation (PDO), a pattern of Pacific climate variability defined by shifting ocean temperature anomalies in the northeast and tropical Pacific Ocean (Latif and Barnett, 1993; Zhang et al., 1997; Minobe, 2000; Mantua and Hare, 2002).

Mean annual temperature at Dillingham, located ~100 km south-east of Shadow Bay (Fig. 1A), is 1°C with monthly mean temperatures ranging from –9°C to 13°C (1971–2000; Western Regional Climate Center (WRCC), 2008). Mean annual precipitation is 645 mm and 50%

of the total falls between July and October as rainfall. Meteorological data for Dillingham (Western Regional Climate Center (WRCC), 2008) include daily surface air temperature and precipitation for a period spanning from 1919–2007.

A meteorological station equipped with an Onset HOBO temperature/relative humidity sensor and rain gauge was established at Shadow Bay in August 2006 (data at http://jan.ucc.nau.edu/~dsk5/S_AK/). A comparison of mean daily air temperature (August 2006–2007) with Dillingham shows a strong correlation ($r^2 = 0.95$, $n = 364$, $p < 0.0001$), suggesting that meteorological conditions at Shadow Bay are similar to the regional climatology. Rainfall at Shadow Bay is less closely related to that at Dillingham ($r^2 = 0.59$, $n = 131$, $p < 0.0001$), likely due to local factors typical of mountainous terrain. Similarities

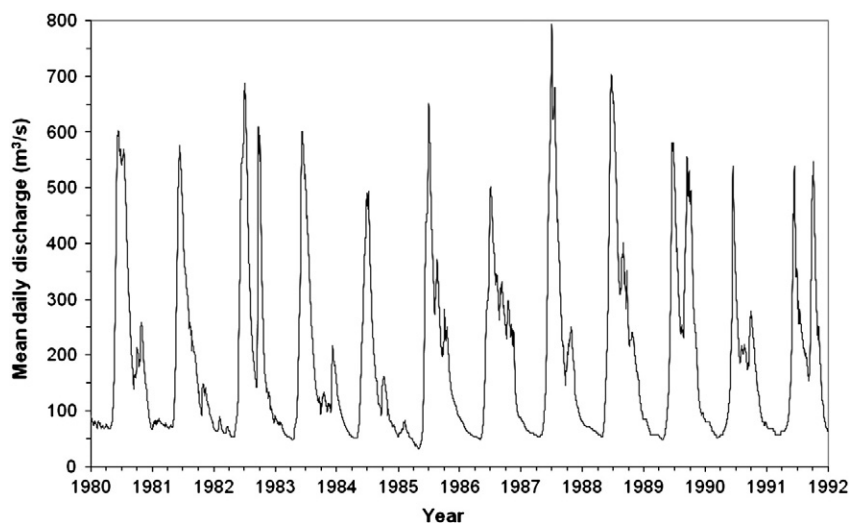


Figure 2. Discharge record from the Nuyakuk River (Station ID 15302000, 59.56°N, 158.11°W) for a period of 11 years (1980–1991; United States Geological Survey (USGS), 2008). This gauging station is located at the outflow of Nuyakuk Lake, approximately 56 km east of Shadow Bay (Fig. 1A).

and differences between the temperature and precipitation at Dillingham compared with Shadow Bay are described elsewhere (Kaufman, 2008).

The longest available streamflow record (1953–2007) is for the Nuyakuk River (United States Geological Survey (USGS), 2008; Fig. 2). Although the Nuyakuk River is likely representative of overall discharge patterns within the Ahklun Mountains, the station gauges the outflow of a large lake (Nuyakuk Lake) ~56 km east of Shadow Bay, and likely exhibits dampened discharge peaks and longer response times to regional weather events compared to the river flowing into Shadow Bay.

Methods

Sediment coring and processing

Five surface sediment cores (7 cm diameter) ranging in length from 35.0 to 56.0 cm were recovered using a gravity corer from the deepest part of Shadow Bay in August 2006 and April 2007 (Fig. 1; Table 1). In all but one core (06-SB-2A), the sediment-water interface was well-preserved. Cores were stabilized vertically for at least two days and dewatered before topping with hydrophilic foam to minimize disturbance during transport.

In the laboratory, cores were split lengthwise, logged, photographed, and one half of each was archived. Overlapping sediment monoliths were sampled for thin sections using metal trays (7 × 1.5 × 0.5 cm), wrapped in paper towel to prevent collapse of sedimentary structures during dehydration, freeze-dried, and impregnated with a single application of Spurr's low-viscosity epoxy resin under low vacuum (Lamoureux, 2001). Sections were ground to transparency suitable for optical microscopy. Transmitted-light images of the thin sections were obtained using a flatbed scanner at 2400 dpi. Prior to embedding, selected monoliths were X-rayed with a Siemens medical X-ray machine to differentiate thin (<1 mm) minerogenic layers based on density differences (Tiljander et al., 2002).

Laminae were identified using optical microscopy and a master chronology was generated by compilation of the thin-section scans using CoreDRAW 10.0. Adjacent images were correlated using prominent marker beds with distinctive sedimentary characteristics (Lamoureux, 2001). X-radiographs were used to help verify varve delineation. Laminae were identified independently by two of the authors (CAK and SFL) to assess reproducibility. Sedimentary structures were measured using a Velmex measurement stage (0.001 mm resolution). The thickness of each lamina was measured in three positions on the thin sections and the results were averaged (± 0.210 mm).

Surface cores 06-SB-2A, 07-SB-1A, 07-SB-2A/B, and 07-SB-3B were subsampled for grain-size analysis at 1 mm depth intervals. Organic matter was removed by repeated applications of 30% H₂O₂ over a two-week period, then clay colloids were dispersed in a solution of sodium hexametaphosphate. The 918 samples were sonicated for 60 s and analyzed three times for 60 s on a Beckman Coulter LS200 laser diffraction particle size analyser. Mean coefficients of variation (COV, standard deviation divided by the mean) for six duplicate sample pairs were used to evaluate the precision of grain-size analysis and results differed by less than 10% for mean and modal grain size,

indicating the reproducibility of the procedure. All four instrument and eight analytical blanks analyzed were below instrument detection limits.

Varves could not be sub-sampled individually because of their complex internal structure that could often only be distinguished using microscopy. The regular sampling interval used for grain-size analysis crossed varve boundaries, but was converted to a temporal scale using average varve thicknesses and by accounting for shifts in mean varve thickness related to regime shifts (discussed below). The assignment of grain-size values to a time scale may be slightly incorrect in places, but the approach was deemed the best possible under the circumstances.

The upper 20 and 25 cm of surface core 06-SB-2B was sampled for ²³⁹⁺²⁴⁰Pu and ¹³⁷Cs dating, respectively. These radionuclides are associated with nuclear weapons testing and the interval of peak fallout corresponds with 1963–1964 (Ketterer et al., 2004). Samples were taken at 1 cm intervals, dried overnight at 50°C, and ground with a mortar and pestle. They were analyzed for Pu isotopes at the Department of Chemistry and Biochemistry, Northern Arizona University using Inductively Coupled Plasma Mass Spectrometry. ¹³⁷Cs was analyzed on an Ortec high-purity gamma spectrometer in the Department of Biology at Queen's University. Samples were also analyzed for ²¹⁰Pb, but could not be used for geochronology as unsupported Pb activity in all samples was below instrumental background levels.

Varve thickness, grain size, and hydroclimatological datasets were analyzed for regime shifts using Sequential Regime Shift Detector version 3.4 using red-noise estimation and pre-whitening options (Rodionov, 2004, 2005; <http://www.climatologic.com>). The program uses a sequential algorithm to identify shifts above or below the mean of a user-defined cut-off length (similar to a low-pass filter) and threshold significance level. The program does not require an *a priori* assumption of the timing of regime shifts and can distinguish regimes from Gaussian red noise processes (Rodionov et al., 2005).

Results¹

Sedimentology and chronology

Sediment recovered from Shadow Bay cores is composed entirely of rhythmically laminated inorganic sediments. In thin section, the rhythmites consist of one to four silt units overlain by a distinct clay cap. Silt units grade into the overlying clay lamina, while the upper contact of clay units is abrupt and distinct. Some clay caps contain thin partings of silt. Laminae thicknesses average 2.81 mm and range from 0.38 to 25.80 mm (Fig. 3), while modal grain size averages 9.4 μm and ranges from clay (1.6 μm) to very fine sand (80.1 μm; Fig. 5). Angular granules (2.0 to 6.0 mm diameter) mark the lower contact of some silt units (Fig. 6). These granule-rich layers were likely transported onto the lake-ice surface by avalanches and deposited during the spring thaw. The presence of inferred avalanche debris offers additional evidence for divisions between annual sedimentary units. Visible organic matter consisting of woody debris, seeds, and spores are apparent at a depth of 54.1 cm and at the base (83.4 cm) of core 06-SB-2A.

Inter-core comparison of granule layers, laminae structures, and anomalously thick marker beds were used to cross-correlate cores and generate a master chronology (Fig. 3). Sedimentary structures are well-preserved in all cores, with the exception of a 1.57-cm-thick section spanning 46.1 to 47.6 cm depth in core 06-SB-2A, which was disturbed during transport. The regular rhythmicity of the sediments and consistent recurrence of distinct clay layers, in combination with

Table 1

Meta data for sediment cores used in this study. Note that all cores were collected from within 5 m of each other.

Core identification	06-SB-2A	06-SB-2B	07-SB-1A	07-SB-2B	07-SB-3A
Year collected	2006	2006	2007	2007	2007
Coordinates	60.0096° N, 159.1822° W				
Water depth (m)	69.2				
Core length (cm)	66.0	48.2	19.5	28.0	18.0

¹ Varve type, thickness, and grain-size datasets are provided in Appendix A and online at the World Data Center for Paleoclimatology, <http://www.ncdc.noaa.gov/paleo/paleo.html>.

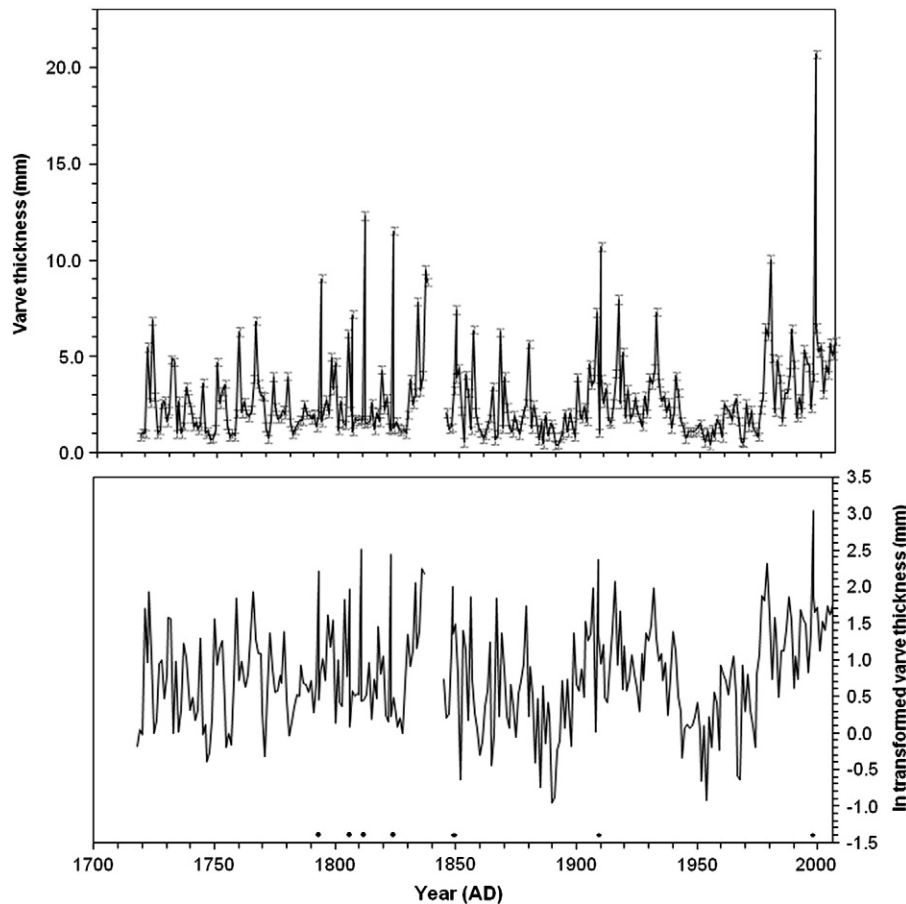


Figure 3. Varve thickness series from Shadow Bay sediments (upper panel). Grey bars show the range of thicknesses measured for each varve. Thicknesses have been ln-transformed to accentuate low-frequency variability and satisfy assumptions of normality necessary for statistical analysis (lower panel). The chronological gap between AD 1837–1855 is due to core disturbance during transport. Dots along x-axis denote anomalously thick units interpreted as turbidites.

the strong seasonality of the regional hydrometeorological regime (Fig. 2) suggest that laminated sediments from Shadow Bay are likely varves. This interpretation is supported by the peak activities of ^{137}Cs and $^{239+240}\text{Pu}$ that coincide with the couplet assigned to 1963 (Fig. 4). Our Shadow Bay chronology covers a period of 289 ± 3 years, from AD 1718 to 2006. The sediments are too young for radiocarbon dating and no tephtras were found to aid in the geochronology.

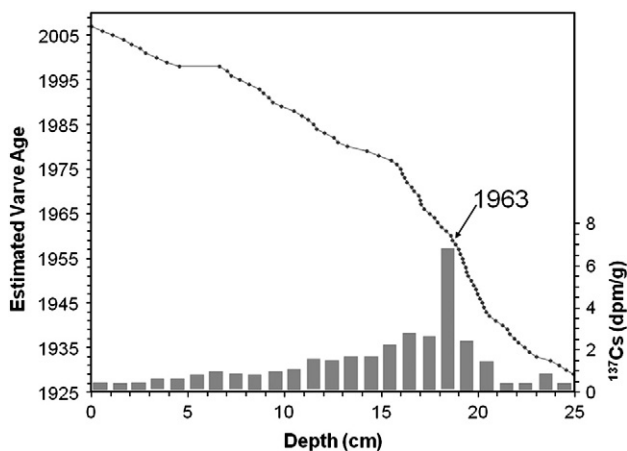


Figure 4. Comparison of varve counts and ^{137}Cs (grey bars) and $^{239+240}\text{Pu}$ (solid line) profiles obtained from surface core 06-SB-2A.

Subannual sedimentary analysis and varve classification

Sedimentological criteria were used to classify varves according to their internal structure (Table 2). The intra-varve structures were compared with the available discharge record (1953–2007) from the Nuyakuk River to relate subannual stratigraphy to the annual hydrograph. This approach has been employed successfully in other studies (i.e. Cockburn and Lamoureux, 2007; Chutko and Lamoureux, 2008; Menounos and Clague, 2008).

Type A varves are the most common type (42%). They consist of one normally graded silt unit overlain by a distinct clay cap. These units generally correspond to years when the annual hydrograph was dominated by the spring snowmelt flood and the fall discharge peak was minimal (Table 2).

Type B varves consist of one or more subannual laminations in the coarse (silt) unit, with the uppermost silt unit grading into the clay cap, and they account for 12% of the varves. Varves of this class are usually present in years when the spring-melt portion of the hydrograph contained multiple peaks (Table 2), although multiple weeks between flow peaks were probably necessary to generate distinct laminae, as noted elsewhere (e.g. Chutko and Lamoureux, 2008; Menounos and Clague, 2008).

Type C varves are composed of one or more silt units within the clay cap of an individual varve and comprise 19% of the varves. With an abrupt lower contact, these subannual laminations interrupt the formation of the clay cap and are interpreted as the product of high flows generated by autumn storms. Type C varves generally correspond to years with distinct fall discharge peaks in the Nuyakuk River record (Table 2). However, when spring and fall discharge peaks

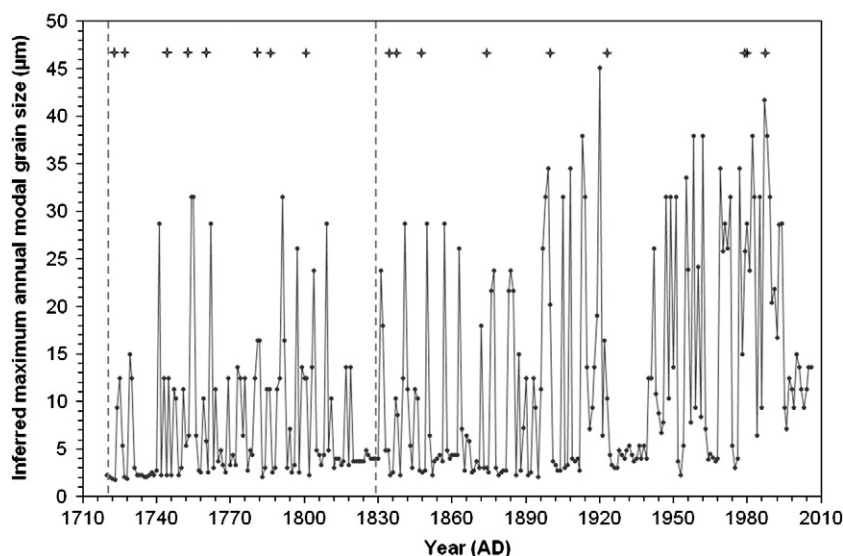


Figure 5. Maximum grain size based on Shadow Bay cores 06-SB-2A, 07-SB-1A, 07-SB-2A/B, and 07-SB-3B. Crosses along top denote years containing angular granules interpreted as avalanche deposits. Dashed grey lines denote location of organic debris.

were of similar magnitude (e.g. 1982) (Fig. 2), the varve structure more closely resembles Type B.

Type D varves, comprising 25% of the sedimentary sequence, contain multiple subannual laminations marked by coarse grains throughout the varve and/or tend to have clay caps with indistinct upper contacts. These units commonly correspond to years in the Nuyakuk River record with a complex series of flow peaks and years with high winter discharge (Table 2). Evidence from sediment traps deployed in Shadow Bay suggests that winter storms and increased air temperatures produced by maritime air mass incursions generated river inflow during the winter of 2006 (Kaufman, 2008).

Seven abnormally thick, graded units were identified and interpreted as turbidites. These Type E varves are substantially thicker (11.27 ± 4.60 mm) than other types (Table 2). The lower contacts of all turbidites show no evidence for erosion; these events probably did not significantly rework underlying sediments or produce gaps in the varve chronology. The assumption that these units are statistical outliers was tested using CLIM-X-DETECT, a program designed to identify extreme events in a time series (Mudelsee, 2006). Using a smoothing parameter (k) of 25, a threshold (z) of 9.5, and a running median of 3 standard deviations, the program identified six of the seven turbidites. The seventh unit is directly below the disturbance gap in the chronology, which likely influenced the CLIM-X-DETECT running median calculation in this region of the time series.

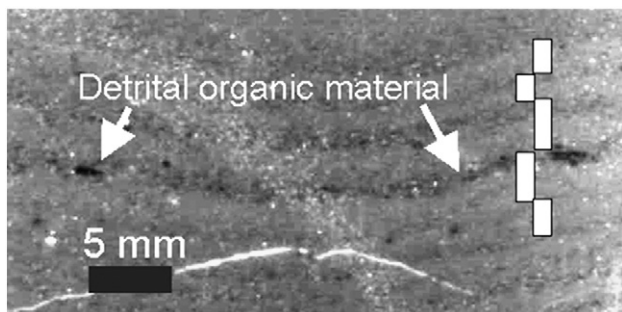


Figure 6. Photomicrograph of 6.2 to 7.8 cm depth in core 07-SB-2B. The granule-rich layer at the lower contact of an individual varve likely represents clastic material transported onto the ice surface by avalanches in the winter and deposited during spring melt. Alternating grey and white bars denote varve boundaries; arrow highlights granule deposit.

Comparison of sedimentary record to hydrometeorological data


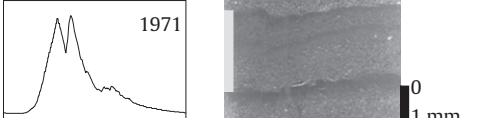
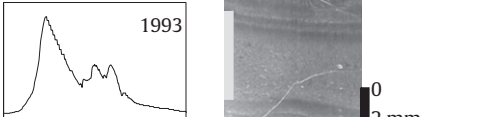

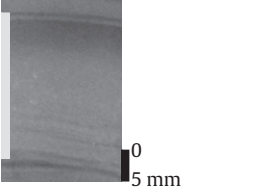
Following the removal of Type E units, varve thickness and maximum grain size were compared with the discharge record from the Nuyakuk River, along with climate variables and indices hypothesized to influence depositional processes in Shadow Bay (Table 3), either by controlling melt-season characteristics (spring temperature, winter temperature and precipitation) or fall discharge (autumn precipitation). The North Pacific index (NP; Trenberth and Hurrell, 1994), a measure of Aleutian Low intensity, and the Pacific Decadal Oscillation index (PDO; Mantua et al., 1997), were also included in the analysis as potential regional indices that would have impacts on the Shadow Bay hydroclimate system. Positive (negative) NP standardized values correspond to a weakened (strengthened) Aleutian Low (Trenberth and Hurrell, 1994), while the warm/positive (cold/negative) phase of the PDO is associated with a deepened (weakened) Aleutian Low (Mantua et al., 1997). For these analyses, varve thickness was natural-log (\ln) transformed to normalize the data for correlation purposes. Of the varve characteristics tested, \ln -transformed varve thickness is most strongly dependent on total annual discharge ($r^2 = 0.75$, $n = 43$, $p < 0.0001$), while maximum annual grain size is dependent on both maximum mean daily discharge ($r^2 = 0.61$, $n = 43$, $p < 0.0001$) and maximum spring (April–June) discharge ($r^2 = 0.63$, $n = 43$, $p < 0.0001$). Annual varve thickness is poorly correlated with maximum annual grain size ($r^2 = 0.004$, $p = 0.334$).

The relation between Nuyakuk River discharge and different climate variables at Dillingham was also explored (Table 3). Neither total annual discharge nor maximum spring discharge is significantly related to the climate variables tested. Maximum spring discharge is related to total annual discharge ($r^2 = 0.56$, $n = 34$, $p < 0.0001$) and spring melting degree days (MDD; $r^2 = 0.48$, $n = 34$, $p < 0.0001$).

Regime-shift analysis

Varve thickness and modal grain size vary at interannual to multidecadal timescales in the Shadow Bay sequence (Fig. 5). Regime shift analysis was used to test for significant changes in both sedimentological and hydrometeorological datasets over multidecadal timescales. With a threshold significance level (p) = 0.01 and cut-off length (l) = 20, six significant shifts in \ln -varve thickness were identified for the 287 year record (Fig. 7A), and the most significant

Table 2
Varve types, characteristics, and relation to the Nuyakuk River discharge record (AD). Grey bars denote annual limits of varve. An example hydrograph is provided to illustrate the inferred hydrological conditions that resulted in the corresponding varve structure.

Varve Type	Description	Mean thickness \pm std dev (mm)	Hydroclimatological interpretation	Sample Nuyakuk River hydrograph and corresponding varve
A	Normally graded silt with distinct clay cap	2.71, 2.24	Hydrograph dominated by continuous spring melt	
B	Subannual laminations in coarse (silt) unit	2.57, 1.65	Episodic spring melt and/or enhanced storm activity facilitates additional pulse of sediment to lake	
C	Subannual laminations in fine (clay) unit	2.61, 1.69	Spring melt dominates hydrograph, secondary sediment inputs from fall storms	
D	Subannual laminations throughout unit and/or indistinct upper contact	3.04, 1.89	Hydrograph contains complex series of peaks and may include enhanced winter discharge	
E	Abnormally thick, normally graded unit	11.27, 4.60	Turbidite	n/a 

shift occurred in 1976. Varves were thicker between: AD 1829–1854, 1899–1941, and 1976–2006, and thinner between AD 1718–1828, 1855–1898, and 1942–1975. Between AD 1829 and 2006, the mean interval between regime shifts was 35.6 ± 7.8 years. Prior to 1829, In-varve thicknesses were consistently thinner than the long-term mean. In contrast to varve thickness, grain-size changes do not show a coherent pattern of multidecadal variability.

The number and magnitude of phase shifts identified in a time series depends on the choice of cut-off length. Using the criteria discussed above (Fig. 7A), no phase shifts were identified in Shadow Bay varve thickness time series between AD 1718 and 1828. Reanalyzing the time series using a reduced cut-off length ($l=10$, $p=0.1$), four regime shifts were identified during this interval (Fig. 7B). All regime shifts subsequent to AD 1829 detected during

Table 3
Coefficients of determination (r^2) calculated for least-squares regression analysis of ln-transformed varve thickness, maximum annual modal grain size, and Nuyakuk River discharge (March 1 water year) against various hydrometeorological variables. Highly significant r^2 values are denoted in bold type.

Variable	Ln-transformed varve thickness		Max grain size		n	Total annual ¹ discharge ²		Maximum spring (Apr–Jun) discharge ²		n
	r^2	<i>p</i> -value	r^2	<i>p</i> -value		r^2	<i>p</i> -value	r^2	<i>p</i> -value	
Total annual ¹ discharge ²	0.75	<0.0001	0.34	<0.0001	43	–	–	–	–	–
Maximum mean daily discharge	0.28	<0.001	0.61	<0.0001	43	–	–	–	–	–
Maximum spring (Apr–Jun) discharge	0.27	<0.001	0.63	<0.0001	43	0.56	<0.0001	–	–	34
Spring melting degree days (MDD) ³	0.00	0.917	0.02	0.358	63	0.02	0.426	0.00	0.833	34
Winter (Nov–Mar) MDD	0.02	0.426	0.01	0.413	52	0.03	0.362	0.00	0.736	30
Total annual precipitation ³	0.02	0.304	0.01	0.549	48	0.03	0.350	0.03	0.357	31
Total autumn (Aug–Oct) precipitation	0.00	0.928	0.01	0.457	58	0.01	0.680	0.01	0.649	34
Total winter precipitation	0.03	0.221	0.02	0.370	50	0.13	0.040	0.06	0.177	33
Average winter NP ⁴	0.07	0.006	0.01	0.417	106	0.14	0.015	0.08	0.059	43
Average winter PDO ⁵	0.12	<0.001	0.01	0.536	107	0.13	0.018	0.04	0.134	43
Maximum annual grain size	0.004	0.334	–	–	287	–	–	–	–	–

¹ Annual discharge = March 15–March 14.

² Nuyakuk River discharge (Station ID 15302000; United States Geological Survey (USGS), 2008).

³ Air temperature and precipitation data from Dillingham Airport (Western Regional Climate Center (WRCC), 2008).

⁴ Trenberth and Hurrell, 1994.

⁵ Mantua et al., 1997.

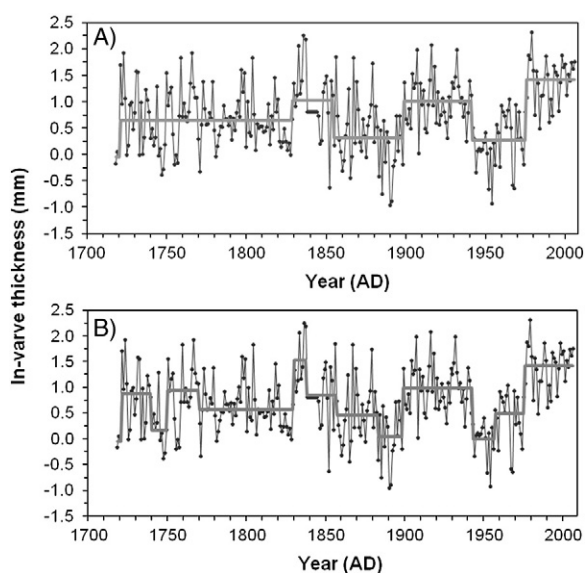


Figure 7. Multidecadal regime shifts (grey line) identified using the sequential method (Rodionov, 2004) for the entire Shadow Bay In-transformed varve thickness time series (AD 1718–2006). Results using (A) a cut-off length (l) = 20, p = 0.01, and (B) l = 10, p = 0.1.

the initial analysis were also identified with the reduced cut-off length, but transitions occurred step-wise instead of as single shifts.

Other hydroclimatic time series were also analyzed for regime shifts (Fig. 8). Of these, regime shifts were identified only in the mean winter NP and PDO indices (p = 0.1, l = 20). Transitions between periods of overall strong and weak Aleutian Low occurred in 1924, 1947, and 1977, and closely coincided with transitions between warm and cool PDO phases. These shifts agree with published values (Mantua and Hare, 2002; Rodionov et al., 2007). In 1977, a significant (p = 0.1, l = 10) shift to higher discharge values was also identified in the relatively short Nuyakuk River record.

Discussion

Varve thickness as a proxy for annual streamflow

In regions where interannual weather patterns can vary dramatically, linking sedimentary proxies to individual climate variables is difficult (Cockburn and Lamoureux, 2007; Hodder et al., 2007). This is the case for Shadow Bay where sedimentological parameters do not show significant relations to annual climate variables (Table 3). In this transitional climate, varve formation is likely shaped by many variables (precipitation, snowpack development, length and intensity of spring melt, glacial melt, etc.). Instead of single variables, hydrological responses integrate multiple climate variables, an intermediary between climate and lake sedimentation. The fact that the Shadow Bay varve record best relates to Nuyakuk River discharge (Table 3) suggests that this river effectively integrates multiple climatic conditions in the Ahklun Mountains. Similar to sedimentological parameters, Nuyakuk River discharge does not relate significantly to individual climate variables over interannual timescales.

Our finding that varve thickness at Shadow Bay depends on total annual discharge rather than peak discharge suggests that sediment transport to the lake is not limited to the spring snowmelt period, and that flows generated by fall storms contribute substantially to sediment transport. Similar to Shadow Bay, varve thickness was correlated with total annual discharge at Lillooet Lake, British Columbia located at 50° 14.59' N (Gilbert, 1975), where annual discharge patterns are similar to those in the Nuyakuk River. In contrast, in mid-central Sweden, discharge regularly peaks during

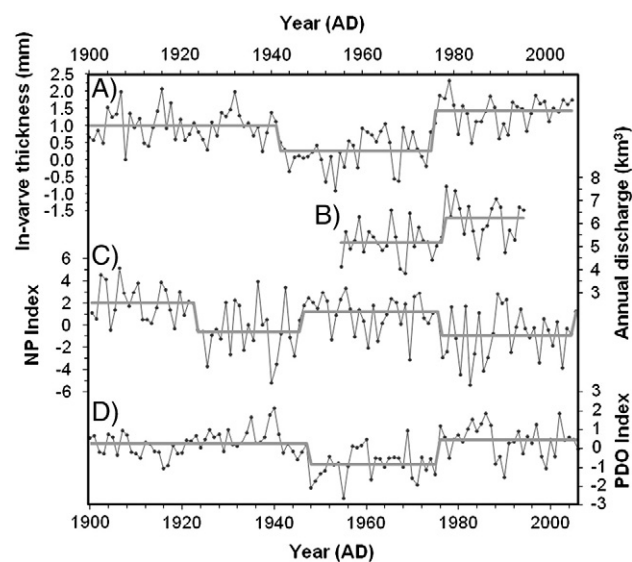


Figure 8. Multidecadal regime shifts (dark grey lines) identified using the sequential method (Rodionov, 2004) for (A) Shadow Bay In-transformed varve thicknesses (AD 1718–2006), (B) Nuyakuk River total annual discharge (AD 1954–1995), (C) mean winter (Nov–Mar) North Pacific (NP) index (AD 1901–2006; Trenberth and Hurrell, 1994), and (D) mean winter (Nov–Mar) Pacific Decadal Oscillation (PDO) index (AD 1901–2006, Mantua et al., 1997).

snowmelt floods, and varve thickness in a lake there was correlated (r^2 = 0.77) with maximum annual discharge rather than with total discharge (Sander et al., 2002).

Grain size as a proxy for maximum spring discharge

At Nuyakuk River, maximum annual flows tend to occur during the spring melt period, although secondary peaks associated with rainfall occur during the fall and are of similar magnitude to snowmelt peaks in 39% of the years (Fig. 2) (Kaufman, 2008). We hypothesize that river competence and the maximum grain size transported increase with discharge magnitude. Further, given that maximum discharge is typically associated with the nival freshet, we expect a relation between the maximum grain size in a given varve and spring discharge. Results from this study support this hypothesis; they show that maximum annual grain size in Shadow Bay is significantly correlated with maximum spring discharge. Maximum annual grain size therefore reflects the short-lived conditions associated with peak spring flows and follows similar conclusions by Francus et al. (2002) in a High Arctic setting, while other studies have linked sediment transport and deposition in nival environments to spring temperatures during the snowmelt peak (e.g. Hughen et al., 2000).

Influence of glacial fluctuations on sedimentation

Glacial fluctuations also influence sedimentation in lakes with glaciofluvial input (e.g. Leonard, 1997). For example, glacier expansion during the Little Ice Age (LIA) coincides with the onset of continuous varve sedimentation (Cockburn and Lamoureux, 2005). In the northeastern Ahklun Mountains, glaciers were about twice as large during the LIA compared with the late 20th century, although the timing of advances remains poorly constrained (Levy et al., 2004). The decrease from about 8% ice coverage of the Shadow Bay catchment during the LIA to 4% ice coverage in the 1970's cannot be identified in Shadow Bay varve characteristics. This is consistent with findings from Sunday Lake in the Ahklun Mountains, where lake-sediment evidence for LIA glacier fluctuations was not readily apparent (Levy, 2002). Further, given the limited evidence for major LIA climate changes in the Ahklun Mountains (Levy et al., 2004), we

do not expect that changes in the annual extent of lake ice or changes to lake circulation would alter the primary sediment inflow or deposition dynamics of Shadow Bay.

Using Shadow Bay varves to infer PDO variability

While interannual relations between Shadow Bay varves or Nuyakuk River discharge and regional climate indices are insignificant, visually coherent multidecadal regime shifts are apparent during the instrumental period (Fig. 8). The shift from cold to warm PDO and weak to strong Aleutian Low in 1977 is reflected in the Nuyakuk River discharge record as a shift to increased total annual discharge, and in the varve thickness record as a transition to increased varve thickness (although the shift occurs in 1976). Similarly, the shift from warm to cold PDO and strong to weak Aleutian Low in the mid-1940's is reflected in varve-thickness time series, although the NP and PDO shifted in 1947, whereas the transition to decreased varve thickness occurred in 1945 (Fig. 8). From AD 1900–1947 both the PDO index and the varve thickness regimes remain in positive states and do not show the 1924 regime shift apparent in the NP index (Fig. 8). These 20th-century regime shifts closely coincide with those identified by Wilson et al. (2007) in their 1300-year Gulf of Alaska coastal surface air temperature reconstruction.

Other studies have likewise linked hydrological variability to PDO. For example, in the southern Alaska, the warm PDO phase seems to be associated with warmer winter air temperatures and enhanced moisture advection leading to increased winter precipitation (Neal et al., 2002). Similarly, Bitz and Battisti (1999) found that mass balance of the Wolverine Glacier (near the coast in south-central Alaska) was positively correlated with PDO, which they attributed to enhanced moisture advection during the winter months during warm PDO phases. Hence, given the hydrological control over the formation of varves in Shadow Bay, we interpret that PDO changes on runoff through winter snowfall and summer rainfall result in higher discharge volume and magnitude. This in turn results in changes to sedimentary texture and mass accumulation.

Warm phases of PDO in the historical record (Mantua et al., 1997) and those inferred from the varve thicknesses, coincide with an increase in occurrence of Type D varves and avalanche debris (Table 4). The indistinct upper contacts of clay caps that typify Type D varves suggest that clay deposition during the winter months was interrupted by pulses of sediment and water. These probably reflect above-freezing temperatures caused by warm maritime air-mass incursions that occur in the area (Kaufman, 2008). The increased avalanche debris associated with warm PDO phases suggests warmer winters and increased snowpack at Shadow Bay during these times. It is less clear if warmer PDO phases would reduce, or in some years, prevent the formation lake ice. However, we interpret the avalanche debris in Shadow Bay to have been deposited onto ice with subsequent rafting and deposition at the core site.

Table 4

Frequency of Type D varves and avalanche debris relative to PDO regimes shifts inferred from the Shadow Bay varve record. Type D varves are interpreted to represent years when above-freezing winter air temperatures generated periodic inputs of sediment and water to Shadow Bay.

Reconstructed PDO regime (duration)	Inferred phase	Frequency (%)	
		Type D varves	Avalanche debris
1976–2006 (31)	Warm	32	10
1942–1975 (34)	Cold	15	0
1899–1941 (43)	Warm	30	5
1855–1898 (44)	Cold	11	2
1829–1854 (26)	Warm	47	16
Mean warm phase ± std dev		37 ± 9	10 ± 6
Mean cold phase ± std dev		13 ± 2	1 ± 1

Other studies have investigated long-term trends in PDO and have produced somewhat differing results prior to the 20th century (Fig. 9). For example, Biondi et al. (2001) used a network of tree-ring chronologies for southern and Baja California to infer a bi-decadal weakening in PDO amplitude from the late 1700's to mid-1800's. Similarly, MacDonald and Case's (2005) tree-ring records from opposite ends of the PDO dipole in California and Alberta showed no significant variability within the 50 to 100 year frequency range between AD 1600 and 1800. Prior to the 1850's PDO variability may have been marked by higher-frequency variability (D'Arrigo and Wilson, 2006). Similar to other reconstructions, our varved-based record from Shadow Bay shows reduced PDO shifts prior to the early 19th century (Fig. 9). Our analyses support previous findings that suggest the periodicity of the PDO has varied over time, and that the early 19th century marked a transition to a more frequent or detectable shifts in the PDO (Fig. 9).

Conclusions

The presence of coherent multidecadal regime shifts in the absence of significant interannual variability between annual hydroclimate variables and the Shadow Bay varve record likely reflects the compound relations between large-scale ocean-atmospheric forcing and regional hydroclimate response. The hydroclimate response to climate forcing may be too complicated to identify clear cause-and-effect relations on annual timescales. When these relations are investigated over longer timescales, however, mean shifts in hydroclimate state overshadow the interannual variability. In addition, multidecadal regime shifts are apparent in the time series of Shadow Bay varve thickness and Nuyakuk River total annual discharge, but they are absent in the maximum annual grain size and maximum mean daily (spring) discharge records. Total annual discharge and varve thickness appear to integrate annual weather conditions, whereas maximum discharge and grain size reflect relatively short-lived events. For southwest Alaska, records that integrate climate variables over an entire year or longer seem to capture the multidecadal variability associated with regional atmosphere-ocean processes.

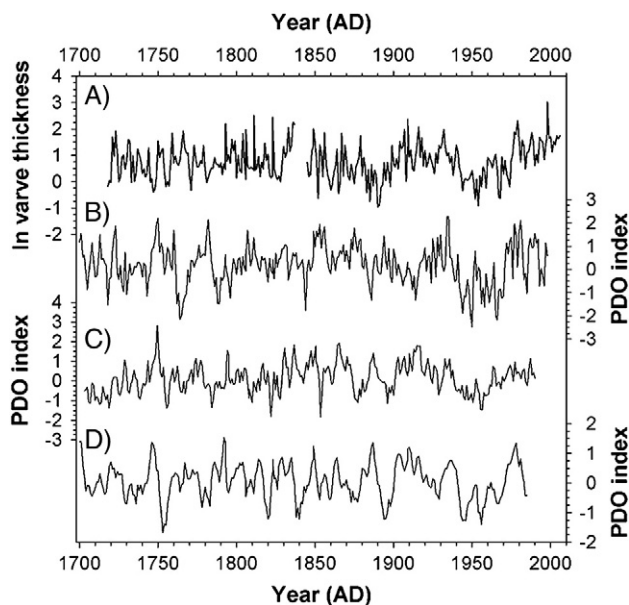


Figure 9. Comparison of (A) Shadow Bay In-transformed varve thickness series with PDO index reconstructions by (B) D'Arrigo and Wilson (2006), (C) Macdonald and Case (2005) and (D) Biondi et al. (2001). Records obtained from the NOAA Data Center for Paleoclimatology (<http://www.ncdc.noaa.gov/paleo/data.html>).

The 289-year-long (AD 1718–2006) sedimentary record from Shadow Bay in combination with instrumental hydroclimate records suggests a complex response to multidecadal climate variability of the North Pacific. Statistically significant relations between varve characteristics and Nuyakuk River discharge suggest that the Shadow Bay varves provide a record of regional discharge variability, while the climate variables tested (e.g. air temperature, precipitation, PDO and NP indices) show little relation to discharge or varve characteristics on interannual timescales. However, on multidecadal timescales, regime shifts in time series of total annual discharge and varve thickness coincide with mean shifts in the NP and PDO indices. On the basis of this coherence, we used varve thickness to reconstruct the timing of PDO regime shifts prior to the 20th century.

Although a number of proxies have been used to reconstruct multidecadal climate variability in the North Pacific, this is the first time that annually laminated sediments have been successfully linked to PDO regime shifts. The investigation of additional varve records from the North Pacific holds potential for understanding the long-term behaviour of this dynamic feature of ocean-atmosphere circulation.

Acknowledgments

We thank C. Grooms and B. Cumming of the PEARL laboratory at Queen's University for assistance with ^{210}Pb dating, M. Ketterer at Northern Arizona University for $^{239+240}\text{Pu}$ analysis, and M. Bollen at Kingston General Hospital for sediment X-radiography. Thanks also to the Dillingham office of the Togiak National Wildlife Refuge and Tikchik Airventures for logistical support, and to R.S. Anderson and A. Werner for their assistance in the field. Comments from two reviewers and the editors improved the manuscript. This research was supported by funding from Queen's University, the Natural Science and Engineering Research Council, Northern Scientific Training Program, Geological Society of America, and National Science Foundation (EAR-0823522).

References

- Biondi, F., Gershunov, A., Cayan, D.R., 2001. North Pacific decadal climate variability since 1661. *Journal of Climate* 14, 5–10.
- Bitz, C.M., Battisti, D.S., 1999. Interannual to decadal variability in climate and the glacier mass balance in Washington, western Canada, and Alaska. *Journal of Climate* 12, 2181–2196.
- Chutko, K.J., Lamoureux, S.F., 2008. Identification of coherent links between interannual sedimentary structures and daily meteorological observations in Arctic proglacial lacustrine varves: potentials and limitations. *Canadian Journal of Earth Sciences* 45, 1–13.
- Cockburn, J.M.H., Lamoureux, S.F., 2005. Timing and climatic controls over Neoglacial expansion in the northern Coast Mountains, British Columbia, Canada. *The Holocene* 15, 619–624.
- Cockburn, J.M.H., Lamoureux, S.F., 2007. Century-scale variability in late-summer rainfall events recorded over seven centuries in subannually-laminated lacustrine sediments, White Pass, British Columbia. *Quaternary Research* 67, 193–203.
- D'Arrigo, R., Wilson, R., 2006. On the Asian expression of the PDO. *International Journal of Climatology* 26, 1607–1617.
- Desloges, J.R., 1994. Varve deposition and the sediment yield record at three small lakes of the southern Canadian Cordillera. *Arctic and Alpine Research* 26, 130–140.
- Francus, P., Bradley, R.S., Abbott, M.B., Patridge, W., Keimig, F., 2002. Paleoclimatic studies of minerogenic sediments using annually resolved textural parameters. *Geophysical Research Letters* 29, 1998–2001.
- Gilbert, R., 1975. Sedimentation in Lillooet Lake, British Columbia. *Canadian Journal of Earth Sciences* 12, 1697–1711.
- Gilbert, R., 2003. Lacustrine sedimentation. In: Middleton, G.E. (Ed.), *Encyclopedia of Sedimentology and Sedimentary Rocks*. Kluwer Academic Publishers, Dordrecht, pp. 404–408.
- Gilbert, R., Crookshanks, S., Hodder, K.R., Spagnol, J., Stull, R.B., 2006. The record of an extreme flood in the sediments of montane Lillooet Lake, British Columbia: implications for paleoenvironmental assessment. *Journal of Paleolimnology* 35, 737–745.
- Hodder, K.R., Gilbert, R., Desloges, J.R., 2007. Glaciolacustrine varved sediment as an alpine hydroclimatic proxy. *Journal of Paleolimnology* 38, 365–394.
- Hughen, K.A., Overpeck, J.T., Anderson, R.F., 2000. Recent warming in a 500-year palaeotemperature record from varved sediments, Upper Soper Lake, Baffin Island, Canada. *The Holocene* 10, 9–19.
- Kaufman, C.A., 2008. Recent hydroclimate dynamics in southwest Alaska: understanding multidecadal climate variability through sedimentary process studies and varve sedimentology. MSc. thesis, Queen's University, Kingston.
- Ketterer, M.E., Hafera, K.M., Jones, V.J., Appleby, P.G., 2004. Rapid dating of recent sediments in Loch Ness: inductively coupled plasma mass spectrometric measurements of global fallout plutonium. *The Science of the Total Environment* 322, 221–229.
- Lamoureux, S.F., 2000. Five centuries of interannual sediment yield and rainfall-induced erosion in the Canadian High Arctic recorded in lacustrine varves. *Water Resources Research* 36, 309–318.
- Lamoureux, S.F., 2001. Varve chronology techniques. In: Last, W.M., Smol, J.P. (Eds.), *Tracking Environmental Change Using Lake Sediments: Basin Analysis, Coring, and Chronological Techniques*, 1. Kluwer Academic Publishers, Dordrecht, pp. 247–260.
- Latif, M., Barnett, T.P., 1993. Causes of decadal variability in the North Pacific and North America. *Science* 266, 634–637.
- Leemann, A., Niessen, F., 1994. Holocene glacial activity and climatic variations in the Swiss Alps: reconstructing a continuous record from proglacial lake sediments. *The Holocene* 4, 259–268.
- Leonard, E.M., 1997. The relationship between glacial activity and sediment production: evidence from a 4450-year varve record of Neoglacial sedimentation near Hector Lake, Alberta, Canada. *Journal of Paleolimnology* 17, 319–330.
- Levy, L.B., 2002. Late Holocene glacier fluctuations, northeastern Ahklun Mountains, southwestern Alaska. MSc. thesis, Northern Arizona University, Flagstaff.
- Levy, L.B., Kaufman, D.S., Werner, A., 2004. Holocene glacier fluctuations, Waskey Lake, northeastern Ahklun Mountains, southwestern Alaska. *The Holocene* 14, 185–193.
- MacDonald, G.M., Case, R.A., 2005. Variations in the Pacific Decadal Oscillation over the past millennium. *Geophysical Research Letters* 32, L08703.
- Mantua, N.J., Hare, S.R., 2002. The Pacific Decadal Oscillation. *Journal of Oceanography* 58, 35–44.
- Mantua, N.J., Hare, S.R., Zhang, Y., Wallace, J.M., Francis, R.C., 1997. A Pacific interdecadal climate oscillation with impacts on salmon productions. *Bulletin of the American Meteorological Society* 78, 1069–1079.
- Menounos, B., 2006. Anomalous early 20th century sedimentation in proglacial Green Lake, British Columbia, Canada. *Canadian Journal of Earth Sciences* 43, 671–678.
- Menounos, B., Clague, J.J., 2008. Reconstructing hydro-climatic events and glacier fluctuations over the past millennium from annually laminated sediments of Cheakamus Lake, southern Coast Mountains, British Columbia, Canada. *Quaternary Science Reviews* 27, 701–713.
- Menounos, B., Clague, J.J., Gilbert, R., Slaymaker, O., 2005. Environmental reconstruction from a varve network in the southern Coast Mountains, British Columbia, Canada. *The Holocene* 15, 1163–1171.
- Minobe, S., 2000. Spatio-temporal structure of the pentadecadal variability over the north Pacific. *Progress in Oceanography* 47, 281–408.
- Mudelsee, M., 2006. CLIM-X-DETECT: A Fortran 90 program for robust detection of extremes against a time-dependent background in climate records. *Computers & Geosciences* 32, 141–144.
- National Oceanographic and Atmospheric Administration (NOAA), 1980. *Climatology of the United States. Monthly normals of temperature, precipitation, and heating and cooling degree days by state, pp. 1951–1980.*
- Neal, E.G., Walter, M.T., Coffeen, C., 2002. Linking the Pacific Decadal Oscillation to seasonal stream discharge patterns in southeast Alaska. *Journal of Hydrology* 263, 188–197.
- Østrem, G., Olsen, H.C., 1987. Sedimentation in a glacier lake. *Geografiska Annaler* 69A, 123–128.
- Rodionov, S.N., 2004. A sequential algorithm for testing climate regime shifts. *Geophysical Research Letters* 31, L09204.
- Rodionov, S.N., Overland, J.E., Bond, N.A., 2005. The Aleutian Low and winter climatic conditions in the Bering Sea. Part I: Classification. *Journal of Climate* 18, 160–177.
- Rodionov, S.N., Bond, N.A., Overland, J.E., 2007. The Aleutian Low, storm tracks, and winter climate variability in the Bering Sea. *Deep Sea Research II* 54, 2560–2577.
- Sander, M., Bengtsson, L., Holmquist, B., Wohlfarth, B., Cato, I., 2002. The relationship between annual varve thickness and maximum annual discharge (1909–1971). *Journal of Hydrology* 263, 23–35.
- Schiefer, E., Menounos, B., Slaymaker, O., 2006. Extreme sediment delivery events recorded in the contemporary sediment record of a montane lake, southern Coast Mountains, British Columbia. *Canadian Journal of Earth Sciences* 43, 1777–1790.
- Tiljander, M., Ojala, A., Saarinen, T., Snowball, I., 2002. Documentation of the physical properties of annually-laminated (varved) sediments at a sub-annual to decadal resolution for environmental interpretation. *Quaternary International* 88, 5–12.
- Trenberth, K.E., Hurrell, J.W., 1994. Decadal atmosphere-ocean variations in the Pacific. *Climate Dynamics* 9, 303–319.
- United States Geological Survey (USGS), 2008. Nuyakuk River (15302000) mean discharge measurements. Available from <http://waterdata.usgs.gov/ak/nwis/2008>.
- Western Regional Climate Center (WRCC), 2008. Dillingham FAA Airport, Alaska: Monthly Climate Summary. Available from <http://www.wrcc.dri.edu/2008>.
- Wilson, R., Wiles, G., D'Arrigo, R., Zweck, C., 2007. Cycles and shifts: 1,300 years of multi-decadal temperature variability in the Gulf of Alaska. *Climate Dynamics* 28, 425–440.
- Wohlfarth, B., Holmquist, B., Cato, I., Linderson, H., 1998. The climatic significance of clastic varves in the Angermanalven Estuary, northern Sweden, AD 1860. *The Holocene* 8, 521–534.
- Zhang, Y., Wallace, J.M., Battisti, D.S., 1997. ENSO-like interdecadal variability: 1900–93. *Journal of Climate* 10, 1004–1019.